

# An Ultra-Thin Triple Band Polarization-Insensitive Metamaterial Absorber for C-Band Applications

Devkinandan Chaurasiya<sup>1</sup>, Somak Bhattacharyya<sup>2</sup>, Saptarshi Ghosh<sup>3</sup>, Praneeth Munaga<sup>4</sup> and Kumar Vaibhav Srivastava<sup>5</sup>

Department of Electrical Engineering  
Indian Institute of Technology, Kanpur  
Kanpur-208016, Uttar Pradesh, India

<sup>1</sup>chaurasiya.dev1189@gmail.com, <sup>2</sup>bhattacharyya.somak@gmail.com, <sup>3</sup>joysaptarshi@gmail.com, <sup>4</sup>praneeth.munaga@gmail.com, and <sup>5</sup>kvs@iitk.ac.in

**Abstract** — An ultra-thin triple band polarization-insensitive metamaterial absorber has been presented in this paper. The unit cell of the proposed structure consists of three concentric rings in the top layer of metal-backed dielectric substrate. The simulated result shows that the proposed structure has triple band absorptivity response lying in C band. The structure exhibits polarization-insensitive behavior under normal incidence due to four-fold symmetry. It also shows high absorption under oblique incidence upto 60° for both TE polarization (above 75%) and TM polarization (above 90%), thus validating the wide angle characteristics. The absorption mechanism is explained through illustrating the electric and magnetic field along with the surface current distribution. The proposed structure has been fabricated and measured, which shows good agreement with simulated response, thus verifying the polarization-insensitivity and wide angle characteristics.

**Index Terms** — Metamaterial, microwave absorber, triple-band absorber.

## I. INTRODUCTION

Metamaterials [1] are artificial composite periodic structures that exhibit exotic electromagnetic properties not occurring in naturally available materials. Due to its significant properties, various research communities of electromagnetic, communication and physics have started extensive research on metamaterials. The various potential applications such as cloaking [2], perfect lens [3], antenna miniaturization [4], perfect absorbers [5] etc. have already been proposed for various frequency ranges using metamaterials. By tailoring the geometrical parameters of metamaterial based absorbers, the structures can be made ultra-thin as well as highly absorptive covering from microwave to optical frequency domain [6-9]. Recently, different types of absorber structures have been proposed providing various characteristics – single band, dual band, multiband, bandwidth-enhanced and broadband applications with polarization-insensitivity and wide angle characteristics [10-15]. The brief explanation regarding the dimensions of the geometrical parameters of metamaterial structures has been discussed by Marques *et al* [16].

In this paper, an absorber structure comprising three concentric rings has been proposed, which shows three different absorption peaks, all lying in C-band. The near-unity absorption occurs at 4.32 GHz, 6.05 GHz and 7.30 GHz with

peak absorptivities of 96.84%, 99.85% and 96.99%, respectively. To understand the physical mechanism of absorption within the structure, the surface current distributions along with electric and magnetic field plots have been presented for all peak absorption frequencies. The proposed structure, being four-fold symmetric, has been found to be polarization-insensitive under normal incidence. It also achieves high absorption for oblique incident angles upto 60° for both TE and TM polarizations. Finally, the absorber structure has been fabricated and measurement has been carried out in anechoic chamber, whose results are closely matched with the simulated responses. The proposed structure is ultra-thin, compact, flexible, polarization-insensitive, wide angle absorptive and thus can be used for various C band surveillance radar applications.

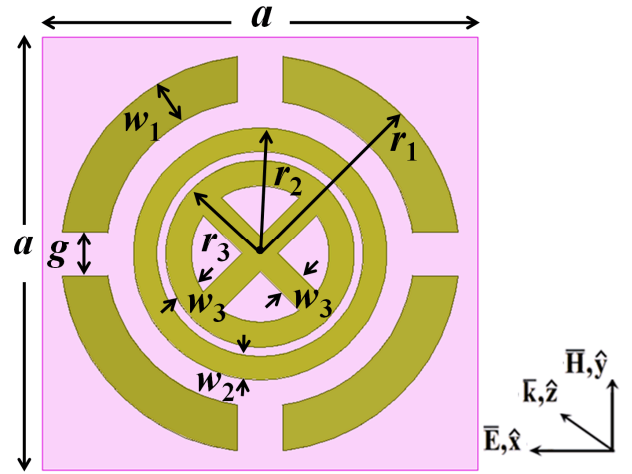


Fig.1. Front view of unit cell geometry of the proposed structure with geometrical dimensions:  $a = 24$  mm,  $r_1 = 11$  mm,  $r_2 = 7$  mm,  $r_3 = 5.2$  mm,  $w_1 = 2.5$  mm,  $w_2 = 1.3$  mm,  $w_3 = 1.4$  mm and  $g = 2.5$  mm.

## II. STRUCTURE DESIGN AND SIMULATED RESULTS

The front view of the unit cell geometry of the proposed structure along with the directions of the field vectors is shown in Fig. 1. The structure has two metallic layers separated by a 1 mm thick dielectric substrate (relative permittivity ( $\epsilon_r$ ) of 4.25 and dielectric loss tangent ( $\tan \delta$ ) of 0.02). The top layer consists of three concentric circular rings, where the outermost

ring is split in four arms, and the innermost ring is cross connected. The bottom layer is completely metal grounded for zero transmission. The optimized geometrical parameters are mentioned in Fig. 1. Both the top and bottom layers are made of copper with conductivity ( $\sigma$ ) of  $5.8 \times 10^7$  S/m and thickness of 0.035 mm.

Since bottom layer is completely copper laminated, transmitted power  $|S_{21}(\omega)|^2$  is zero. Therefore, by proper designing of the structure parameters, reflected power  $|S_{11}(\omega)|^2$  can be minimized. Hence, absorption  $A(\omega)$  within the structure can be maximized as shown in (1)

$$A(\omega) = 1 - |S_{11}(\omega)|^2 - |S_{21}(\omega)|^2 = 1 - |S_{11}(\omega)|^2. \quad (1)$$

The structure is simulated in Ansys HFSS, showing three distinct minima of -15 dB, -28.4 dB and -15.2 dB at 4.32 GHz, 6.05 GHz, and 7.30 GHz respectively, leading to peaks absorptivity of 96.84%, 99.85%, and 96.99% as shown in Fig. 2.

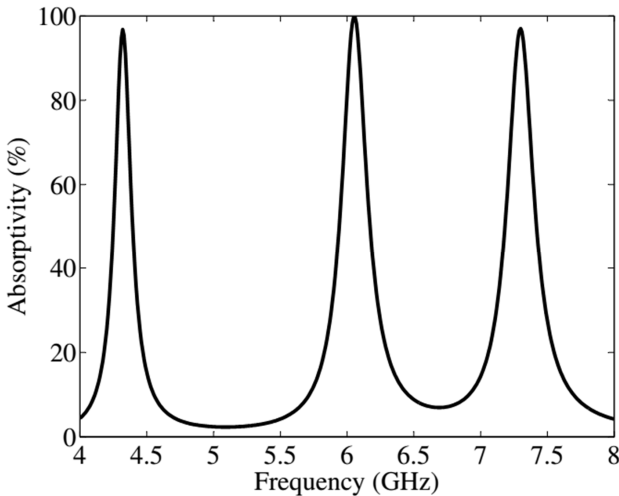


Fig. 2. Simulated absorptivity response of the proposed structure.

Fig. 3 shows the electric and magnetic field distributions at all the absorption frequencies, viz. 4.32 GHz, 6.05 GHz, and 7.30 GHz. It describes the source of electric and magnetic excitations at different portions of the structure at the absorption frequencies. It is observed that at absorption frequencies 4.32 GHz, 6.05 GHz and 7.30 GHz, the middle ring, outer split ring and inner cross connected ring are the primary contributors for highly localized electromagnetic fields respectively.

Fig. 4 shows the surface current distributions at top and bottom layers of the proposed structure to understand the absorption mechanism. It describes that each ring constitutes separate absorption peaks. At 4.32 GHz current is mainly confined within the middle ring, while at 7.30 GHz the current has high density in the inner cross connected ring. The cross in inner ring provides the extra path for flow of current, but due to parallel combination of ring and cross, the effective inductance gets reduced, thereby absorption frequency becomes higher. At the middle frequency 6.05 GHz, surface current is distributed in four arms of the outer split ring. The outer ring, having larger radius, seems to have lowest absorption frequency as compared to the other two smaller rings. But, as seen from the

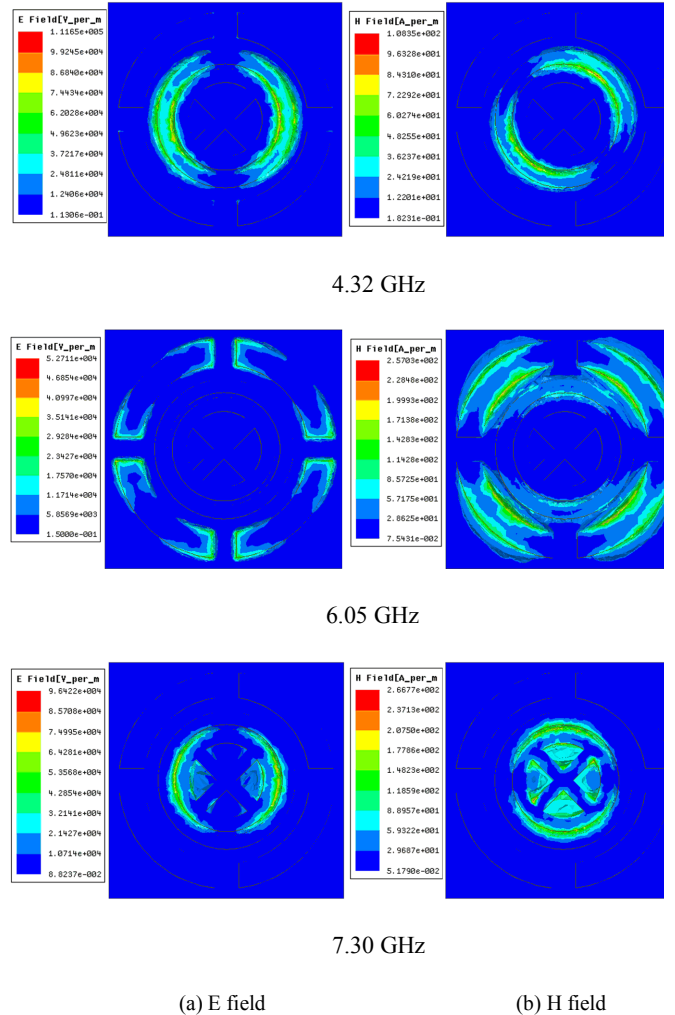


Fig. 3. (a) Electric field distribution and (b) magnetic field distribution at the peak absorption frequencies of the proposed structure.

surface current distribution, the four splits divide the ring into four equal parts; thereby the effective inductance gets reduced. This decreased inductance increases the absorption frequency and therefore, near-unity absorption has been realized at 6.05 GHz.

It is also seen that the direction of surface currents at the top and bottom layers are anti-parallel and therefore, constitute circulating loop perpendicular to the direction of incident magnetic field creating magnetic excitation. On the contrary, induced electric field within the structure is high along the direction of incident electric field, thus creating electric excitation. Therefore, both electric and magnetic excitations occur at absorption frequencies, leading to strong electromagnetic absorption.

The proposed structure has four-fold symmetry and has been found to be polarization-insensitive under normal incidence as shown in Fig. 5. Further, the structure is theoretically examined under oblique incidences for both TE and TM polarizations as shown in Fig. 6, where it shows high absorption (above 75% for TE polarization and above 90% for TM polarization) for incidence angle upto  $60^\circ$ . Beyond that, the absorptivity gradually decreases.

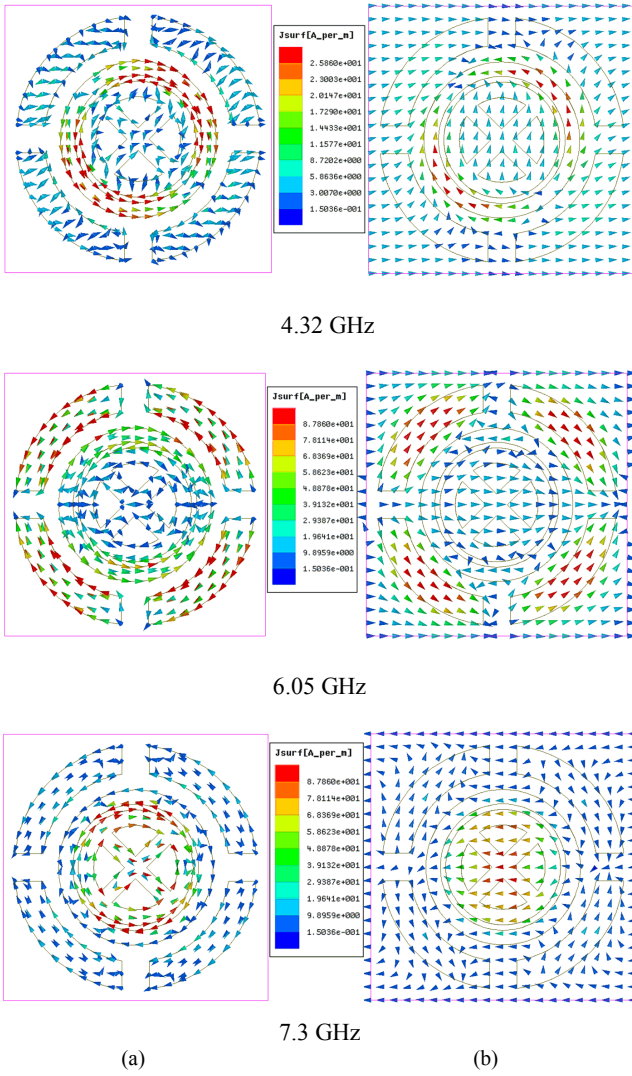


Fig. 4. Surface current distributions at (a) top surface and (b) bottom surface of the proposed structure at the absorption frequencies.

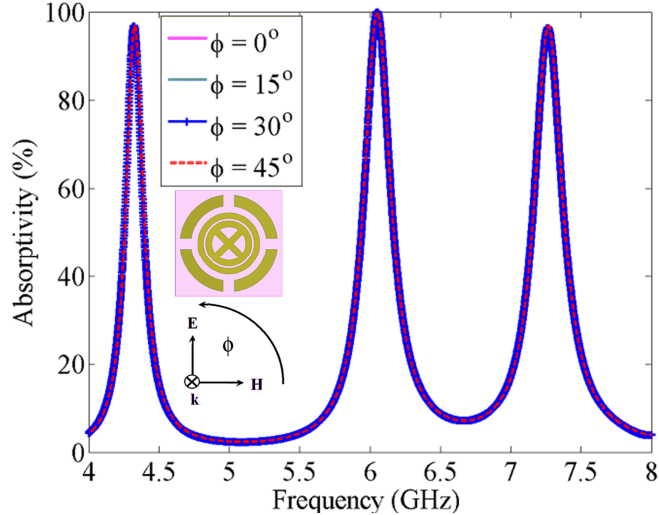


Fig. 5. Simulated absorptivity of proposed structure for different polarization angles under normal incidence.

In order to observe the flexibility property of the triple band absorber, different parameters of the unit cell have been varied in some ranges as shown in Fig. 7. Initially, the radius of the

inner cross connected ring ( $r_3$ ) has been varied from 4.5 to 5.3 mm. It has been observed from Fig. 7(a) that with increasing the radius, the effective inductance value increases and therefore the higher absorption frequency gradually decreases without affecting the response of other two rings. Similarly, by increasing the radii of middle ring ( $r_2$ ) and outer ring ( $r_1$ ), the value of effective inductances increase resulting the corresponding peak absorption frequencies reduced as shown in Fig 7(b) and 7(c) respectively.

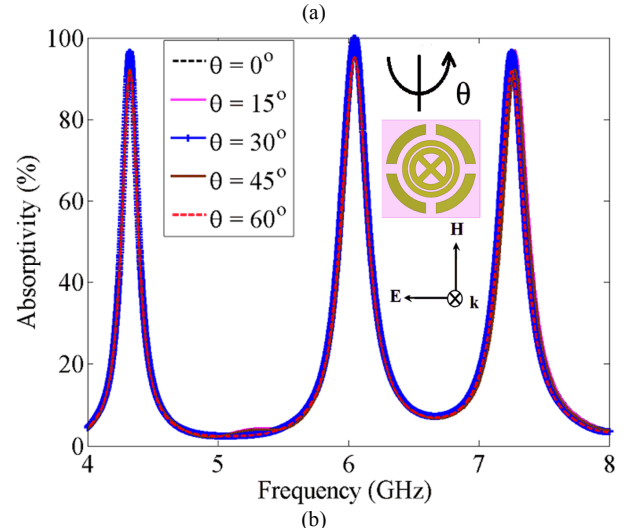
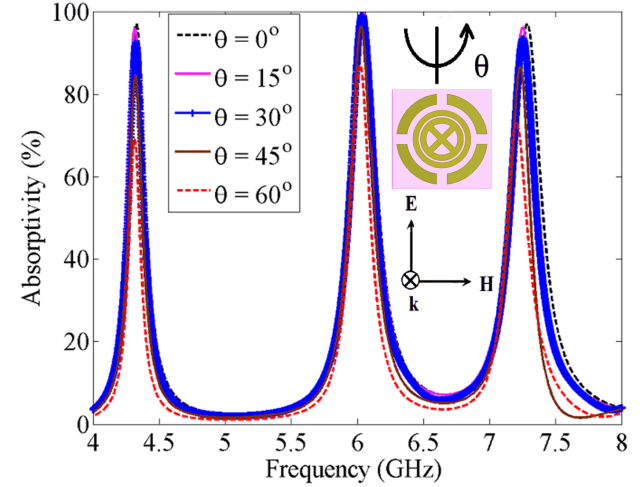


Fig. 6. Simulated absorptivity for different incidence angles under (a) TE polarization and (b) TM polarization of the proposed structure.

Similarly, the parametric variation has been done for gap ( $g$ ) of outer split ring of the proposed structure. It is observed from Fig. 8 that with increase of the gap value ( $g$ ) from 1.5 to 3 mm, the effective metallic patch length decreases, thus decreasing the effective inductance which leads to increase the center absorption frequency. As observed in the figure, the other absorption peaks (lower and higher) remain almost constant with change of the gap ( $g$ ) parameter. As discussed before, the splits in the outer ring divides the ring into equal four parts and the effective inductance gets reduced. Therefore, if the gap has been removed from the outer ring, its absorption frequency will be characterized by a normal ring with radius of 11 mm and the corresponding absorption frequency has been shown in black dotted line in Fig. 8, where the absorption peak in the central one has been shifted to the lowermost absorption peak.

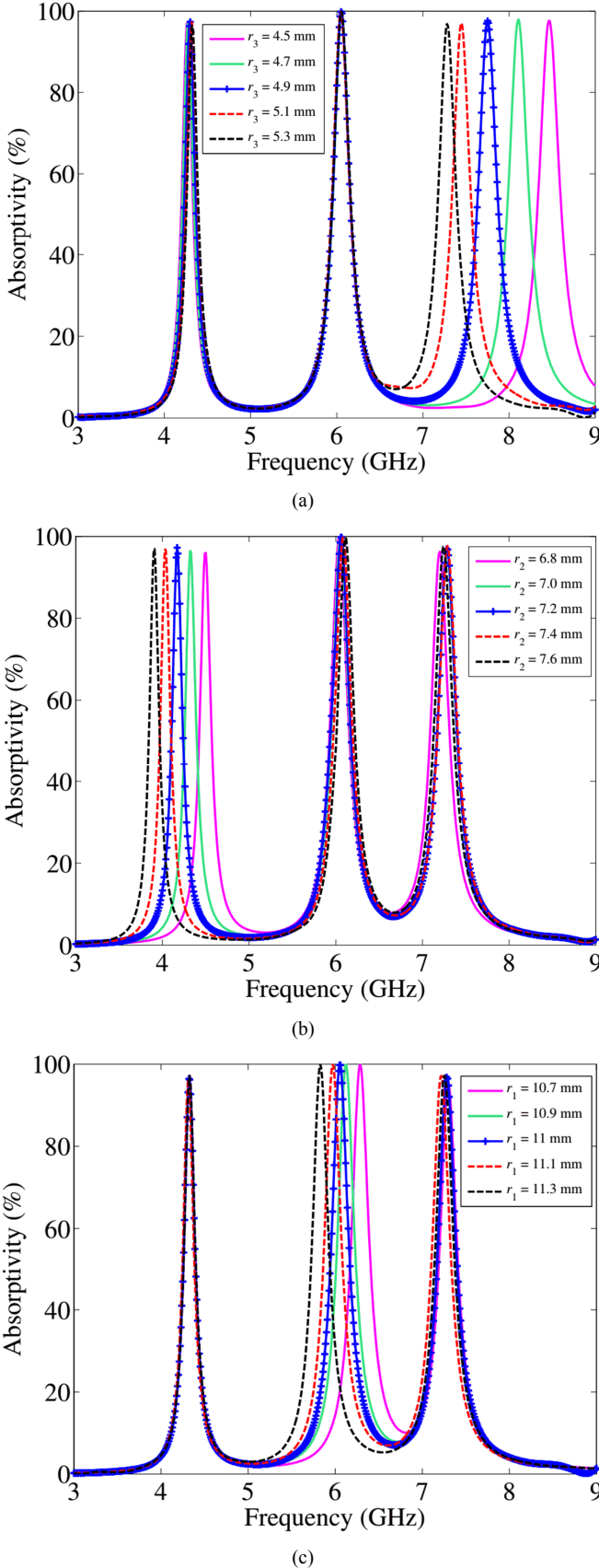


Fig. 7. Simulated absorptivities for different values of radius of (a) inner ring ( $r_3$ ), (b) middle ring ( $r_2$ ) and (c) outer ring ( $r_1$ ) of the proposed structure.

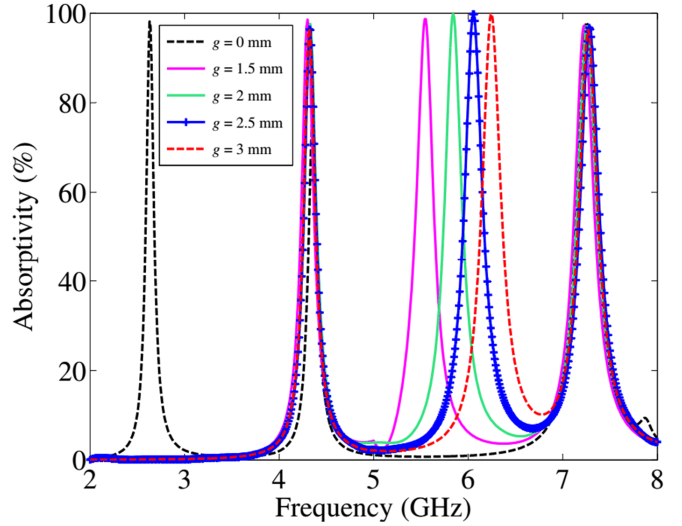


Fig. 8. Simulated absorptivity for different values of gap ( $g$ ) of outer split ring of the proposed structure.

### III. EXPERIMENTAL VERIFICATION

A  $10 \times 10$  unit cells sample has been fabricated on  $240 \text{ mm} \times 240 \text{ mm}$  planar FR-4 substrate (having thickness of 1 mm) as shown in Fig. 9(a) by using printed circuit board (PCB) technology. Fig. 9(b) shows the zoomed view of part of the fabricated structure. The reflected power from the structure has been measured inside the anechoic chamber using two standard horn antennas LB-10180-SF (1-18 GHz) connected with Agilent N5230A vector network analyzer.

Firstly, the reflected power from identical copper sheet has been measured used as a reference level. Then, reflectance from the surface of the fabricated sample has been recorded and the difference between the two reflected powers gives the actual reflection from the structure. The measured result shows absorption peaks at three distinct frequencies 4.33 GHz, 6.10 GHz, and 7.32 GHz with absorptivities of 96.83%, 99.10% and 97.5% respectively. The comparison of simulated and measured absorptivity response is shown in Fig. 10, where good matching is observed except some small deviation in absorption frequencies which could be due to fabrication imperfections.

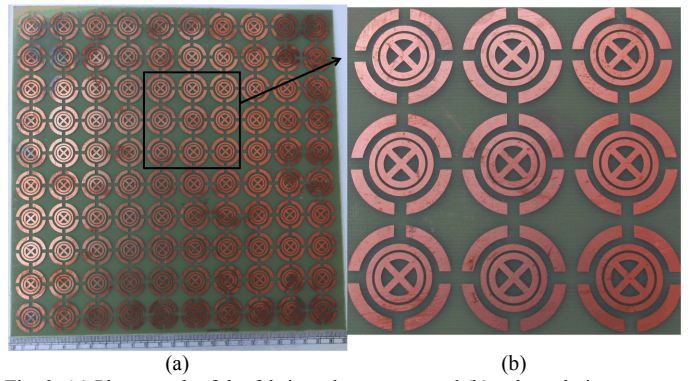


Fig. 9. (a) Photograph of the fabricated structure, and (b) enlarged view.

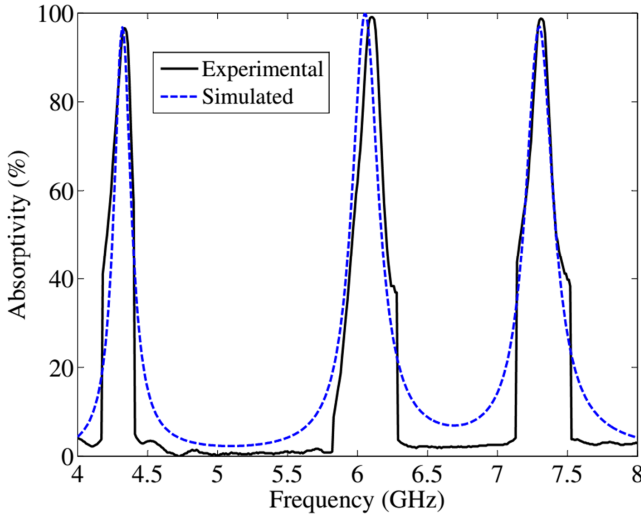


Fig. 10. Comparison of simulated and measured absorptivity under normal incidence of the proposed structure.

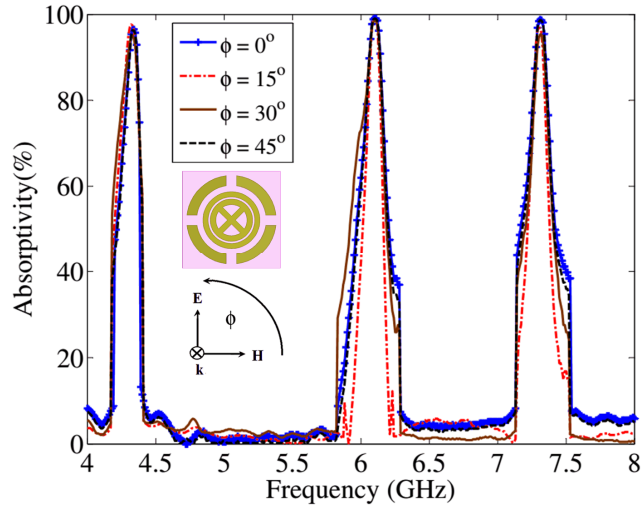
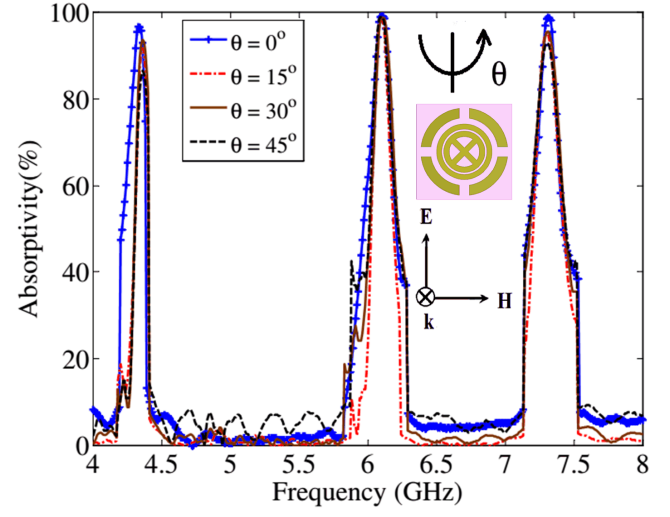


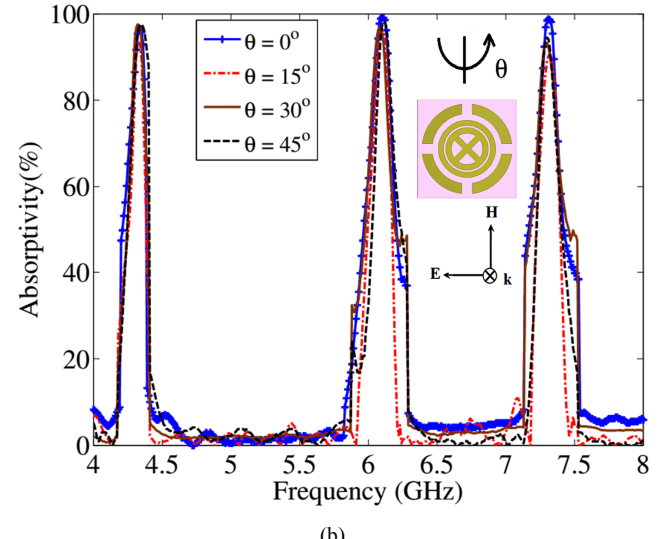
Fig. 11. Measured absorptivity for different polarization angles under normal incidence of the fabricated structure.

The polarization-insensitive behavior of the fabricated structure has been verified by rotating the sample around its axis from  $0^\circ$  to  $45^\circ$ . The rotation has been performed upto  $45^\circ$  due to symmetrical design of the structure. Fig. 11 shows the measured absorptivity response, which shows that the response is almost identical for all polarization angles and is closely matched with simulated response (shown in Fig. 5).

Further, the absorptivity has been measured for different angles of incidence upto  $45^\circ$  for both TE and TM polarizations as shown in Fig. 12(a) and 12(b) respectively. In case of TE polarized wave, the direction of electric field is kept constant while the direction of magnetic field and propagation vector are changed by angle  $\theta$  keeping the sample fixed. Similarly, for TM polarization, the direction of magnetic field is kept constant while the direction of electric field and propagation vector are changed by angle  $\theta$  keeping the sample fixed. The structure provides more than 80% measured absorptivity response in both the cases as evident from Fig. 12. For both the cases the measured responses have good agreement with simulated responses (shown in Fig. 6).



(a)



(b)

Fig. 12. Measured absorptivity for different incidence angles under (a) TE polarization and (b) TM polarization of the fabricated structure.

#### IV. CONCLUSION

An ultra-thin triple band metamaterial absorber has been presented which consists of three concentric circular rings. The dimensions of the rings have been optimized to obtain all three absorption peaks in single microwave band (C-band). In order to understand the physical mechanism of absorption, electric and magnetic field distributions along with surface current distribution have been illustrated for all the peak absorption frequencies. The proposed absorber is polarization-insensitive and highly absorptive for wide incidence angles (upto  $60^\circ$ ) under TE and TM polarizations. Various design parameters have been parametrically analyzed to observe the absorption mechanism of the structure. Finally, the structure is fabricated and experimental measurements have been done to verify the simulated responses. The designed absorber is ultra-thin ( $\sim \lambda/40$  corresponding to the highest frequency), flexible and can be used in many potential applications like air surveillance radar, thermal emitters, wireless communication, phase shifter and defense applications.

#### ACKNOWLEDGMENT

This work partially supported by ISRO, India under Project No. SPO/STC/EE/2014087 and DRDO, India under Project No. DLJ/TC/1025/I/30.

#### REFERENCES

- [1] D. R. Smith, W. J. Padilla, D. C. Vier, S. C. Nemat-Nasser, and S. Schultz, "Composite medium with simultaneously negative permeability and permittivity," *Phys. Rev. Lett.*, vol. 84, pp. 4184-4187, 2000.
- [2] A. Rajput, and K. V. Srivastava, "Design of a two-dimensional metamaterial cloak with minimum scattering using a quadratic transformation function," *J. Appl. Phys.*, vol. 116, no. 12, pp. 124501, 2014.
- [3] K. Saurav, D. Sarkar and K. V. Srivastava, "CRLH Unit-Cell Loaded Multi-Band Printed Dipole Antenna," *IEEE Antennas Wireless Propag. Lett.*, vol. 13, pp. 852-855, 2014.
- [4] S. Enoch, G. Tayeb, and P. Vincent, "A metamaterial for directive emission," *Phys. Rev. Lett.*, vol. 89, pp. 3901-3904, 2002.
- [5] N. I. Landy, S. Sajuyigbe, J. J. Mock, D. R. Smith, and W. J. Padilla, "Perfect metamaterial absorber," *Phys. Rev. Lett.*, vol. 100, pp. 207402, 2008.
- [6] M. H. Li, L. H. Yang, B. Zhou, X. P. Shen, Q. Cheng, and T. J. Cui, "Ultrathin multiband gigahertz metamaterial absorbers," *J. Appl. Phys.*, vol. 110, no. 1, pp. 014909, 2011.
- [7] X. Liu, T. Starr, A. F. Starr, and W. J. Padilla, "Infrared spatial and frequency selective metamaterial with near-unity absorbance," *Phys. Rev. Lett.*, vol. 104, issue 20, pp. 7403, 2010.
- [8] D. Y. Shchegolkov, A. K. Azad, J. F. O'Hara, and E. I. Simakov, "Perfect subwavelength fishnetlike metamaterial-based terahertz absorbers," *Phys. Rev. B*, vol. 82, pp. 205117, 2010.
- [9] K. Aydin, V. E. Ferry, R. M. Briggs, and H. A. Atwater, "Broadband polarization-independent resonant light absorption using ultrathin plasmonic super absorbers," *Nature Comm.*, vol. 2, pp. 517, 2011.
- [10] A. Fallahi, A. Yahaghi, H.-R. Benedickter, H. Abiri, M. Shahabadi, and C. Hafner, "Thin wideband radar absorbers," *IEEE Trans. Antennas & Propag.*, vol. 58, pp. 4051-4058, 2010.
- [11] M.-H. Li, H.-L. Yang, and X.-W. Hou, "Perfect metamaterial absorber with dual bands," *Prog. in Electromag. Res.*, vol. 108, pp. 37-49, 2010.
- [12] S. Bhattacharyya, S. Ghosh and K. V. Srivastava, "Triple band polarization-independent metamaterial absorber with bandwidth enhancement at X-band," *J. Appl. Phys.*, vol. 114, pp. 094514, 2013.
- [13] S. Ghosh, S. Bhattacharyya, Y. Kaiprath and K. V. Srivastava, "Bandwidth-enhanced polarization-insensitive microwave metamaterial absorber and its equivalent circuit model," *J. Appl. Phys.*, vol. 115, pp. 104503, 2014.
- [14] S. Ghosh, S. Bhattacharyya and K. V. Srivastava, "Bandwidth-enhancement of an ultrathin polarization insensitive metamaterial absorber," *Micro. and Opt. Techn. Lett.*, vol. 56, pp. 350-355, 2014.
- [15] H. Xiong, J.-S. Hong, C.-M. Luo, and L.-L. Zhong, "An ultrathin and broadband metamaterial absorber using multilayer structures," *J. Appl. Phys.*, vol. 114, pp. 064109, 2013.
- [16] R. Marques, F. Martin, and M. Sorolla, *Metamaterials with Negative Parameters*(Wiley, New Jersey, 2008), p. 43-90.